AEM
Journals.ASM.org

Screening of *Chlamydomonas reinhardtii* Populations with Single-Cell Resolution by Using a High-Throughput Microscale Sample Preparation for Matrix-Assisted Laser Desorption Ionization Mass Spectrometry

Jasmin Krismer,[a] Jens Sobek,[b] Robert F. Steinhoff,[a] Stephan R. Fagerer,[a] Martin Pabst,[a]* Renato Zenobi[a]

Department of Chemistry and Applied Biosciences, Laboratory of Organic Chemistry, ETH Zurich, Zurich, Switzerland[a]; Functional Genomics Center Zürich, ETH Zurich and University of Zurich, Zurich, Switzerland[b]

The consequences of cellular heterogeneity, such as biocide persistence, can only be tackled by studying each individual in a cell population. Fluorescent tags provide tools for the high-throughput analysis of genomes, RNA transcripts, or proteins on the single-cell level. However, the analysis of lower-molecular-weight compounds that elude tagging is still a great challenge. Here, we describe a novel high-throughput microscale sample preparation technique for single cells that allows a mass spectrum to be obtained for each individual cell within a microbial population. The approach presented includes spotting *Chlamydomonas reinhardtii* cells, using a noncontact microarrayer, onto a specialized slide and controlled lysis of cells separated on the slide. Throughout the sample preparation, analytes were traced and individual steps optimized using autofluorescence detection of chlorophyll. The lysates of isolated cells are subjected to a direct, label-free analysis using matrix-assisted laser desorption ionization mass spectrometry. Thus, we were able to differentiate individual cells of two *Chlamydomonas reinhardtii* strains based on single-cell mass spectra. Furthermore, we showed that only population profiles with real single-cell resolution render a nondistorted picture of the phenotypes contained in a population.

Heterogeneity plays a pivotal role in the emergence of tolerance, persistence, and resistance toward biocides in microbial populations (1, 2). Also, microbial populations show highly complex interactions, e.g., in the competition for nutrients or in the colonization of new habitats (3). In recent years, newly developed tools for single-cell analysis have greatly extended our understanding of biological variation in microbial populations and its underlying mechanisms (4). These tools allow genome sequencing (5) or follow transcription as well as protein synthesis on the single-cell level (6). Since these techniques give a much higher resolution when observing processes in given cell populations, they permit insight into inter- and intracellular processes and the underlying mechanisms. However, when it comes to high-throughput measurements of small molecules, very few methods are currently known (7).

The singular qualities of individual cells can only be fully appreciated within the context of the population. Therefore, one of the most important features for single-cell methods to be useful in biological applications is high-throughput capability. One of the most successful high-throughput approaches to characterize heterogeneities in microbial populations is flow cytometry (8). It has the benefits of high sensitivity and a high linear dynamic range of fluorescence tagging and optical detection. However, the method is strongly limited in parallelization, since excitation and emission bands overlap. Mass cytometry, on the other hand, which is a new approach that can be coupled to flow cytometry, uses antibodies tagged with rare earth metals (9). With mass spectrometric detection, over 40 features can be measured in each cell, implying that mass spectrometry (MS) can boost parallelization capabilities (10).

Unfortunately, labeling small molecular compounds is not possible, because the chemical behavior of low-molecular-weight compounds is heavily affected by the tagging. Furthermore, the selectivity of tags is often determined by the strength of noncovalent interactions specific to an analyte, which can render labeling strategies highly complex. Low-molecular-weight compounds often lack enough distinctive binding motifs to allow for specific binding in complex cellular environments.

On the other hand, some analytes (e.g., molecules with structural functions, such as lipids) are present in much higher copy numbers inside cells than are DNA or proteins, such that they are within the reach of state-of-the-art mass spectrometric detection, as was shown in recent years (11, 12). Matrix-assisted laser desorption ionization (MALDI) imaging mass spectrometry is the method of choice for the analysis of tissues (13), and new laser desorption sources render it possible to image the distribution of small molecules with single-cell resolution (14, 15). Together with its high-throughput capabilities, single-cell MALDI-MS can give

Received 13 April 2015 **Accepted** 2 June 2015

Accepted manuscript posted online 5 June 2015

Citation Krismer J, Sobek J, Steinhoff RF, Fagerer SR, Pabst M, Zenobi R. 2015. Screening of *Chlamydomonas reinhardtii* populations with single-cell resolution by using a high-throughput microscale sample preparation for matrix-assisted laser desorption ionization mass spectrometry. Appl Environ Microbiol 81:5546–5551. doi:10.1128/AEM.01201-15.

Editor: A. M. Spormann

Address correspondence to Renato Zenobi, zenobi@org.chem.ethz.ch.

* Present address: Martin Pabst, PolyTherics Limited, Cambridge, United Kingdom.

Supplemental material for this article may be found at http://dx.doi.org/10.1128/AEM.01201-15.

doi:10.1128/AEM.01201-15

new insights into cell-to-cell variations of low-molecular-weight compounds. However, the applicability of these methods to microbial colonies is a considerable challenge due to the necessity of harsher extraction conditions and the significantly smaller cell size (16).

Here, we present a new method for single-cell-sample workup of microbial cell cultures and their discrete analysis using MALDI-MS. Our method targets the analysis of individual cells in suspension, e.g., cells of microbial cell cultures. As exemplified by using the alga *Chlamydomonas reinhardtii*, the workflow comprises a controlled sample preparation protocol for thousands of individual cells in spatially separated microarray spots that allows the reproducible extraction and analysis of microbial cells despite their robust cell walls (17). Endogenous chlorophyll was detected by MS and by fluorescence measurements. Thereby, each sample preparation step could be monitored optically for optimization. Finally, MS allowed a clear differentiation of two strains of *Chlamydomonas reinhardtii* based on data obtained for each single alga cell. The necessity of true high-throughput single-cell measurements is demonstrated by the deterioration of the characteristic signatures of the two strains when considering multicell spots.

MATERIALS AND METHODS

Chemicals. All solvents were purchased in high-performance liquid chromatography (HPLC)-grade quality. Acetone (Chromasolv), chloroform (ReagentPlus), and isopropanol (Chromasolv) were purchased from Sigma-Aldrich. Water (LiChrosolv) was purchased from Merck. The MALDI matrix 2,5-dihydroxybenzoic acid (DHB) was purchased from Sigma-Aldrich. Hutner's trace elements were purchased from the Chlamydomonas Resource Center (St. Paul, MN, USA).

Cell culture. *Chlamydomonas reinhardtii* strains CC-125 (wild type) and CC-4346 (chlorophyllide *a* oxidase mutant [18]) were obtained from the Chlamydomonas Resource Center, St. Paul MN, USA. Strains were maintained on Tris-acetate-phosphate (TAP) agar plates. For single-cell MS, single colonies of strains were inoculated into liquid TAP medium (19). The cells were cultured in an incubation shaker (Minitron; Infors HT) at 21°C at 110 rpm and 1,200-lx continuous illumination.

Characterization of *Chlamydomonas reinhardtii* strains. The *Chlamydomonas reinhardtii* strains were characterized at the population level using UV-visible light (VIS) spectrometry. Absorption was measured between 350 nm and 850 nm. In UV-VIS spectra, the chlorophyll *a* oxygenase (CAO) insertional mutant strain CC-4346 lacks the characteristic shoulder peaks at around 660 nm and 500 nm caused by chlorophyll *b* absorption.

Microarrays. The microarray for mass spectrometry (MAMS) targets were prepared as follows. Stainless steel target slides, 25 mm by 75 mm, were structured using picosecond laser pulses. Before use, a slide was cleaned using a sequence of different solvent conditions, as follows: (i) chloroform, (ii) acetone, (iii) isopropanol, (iv) 15% acetic acid in water, and (v) water. Each of the conditions was maintained for at least 60 min in a sonication bath. The slides were stored under a nitrogen atmosphere until use.

Spotting the cells onto microarray slides. For liquid handling in nanoliter volumes, a spotting robot (sciFLEXARRAYER S11; Scienion) was used. For single-cell MS, *Chlamydomonas reinhardtii* strains were centrifuged just before spotting at 2,000 × *g*/1,500 × *g* for 5 min (Eppendorf 5415R centrifuge) and resuspended 3 times in deionized water to reduce the quenching influence of salts contained in the TAP liquid culture medium. After spotting the cells, the slide was scanned using a confocal microarray scanner (LS400; Tecan). Fluorescence was excited at 633 nm and detected at 670 nm. The detector gain was kept constant for all measured slides for comparing relative intensities. The scan resolution was 6 μm.

Cell lysis and MALDI matrix application. To enhance extraction and cocrystallization of the analytes with the MALDI matrix (2,5-dihydroxybenzoic acid) while avoiding cross-contamination between microarray spots, the slide was submerged in liquid nitrogen. The slide was reconstituted to room temperature in a desiccator to avoid condensation. A fluorescence scan of the slide was performed after reconstitution to check for possible cell displacements or cross-contamination. After this step, 2,5-dihydroxybenzoic acid (10 mg/ml in 80% aqueous acetone) was spotted onto the cells to extract the analytes and cocrystallize them with the MALDI matrix. The efficiency of the extraction was monitored with a confocal fluorescence scan. The slide was stored under nitrogen atmosphere at −80°C until measured.

MALDI-FT-ICR-MS. Accurate mass spectra of single cells and cells in bulk were recorded using a Fourier transform (FT)-ion cyclotron resonance (ICR) mass spectrometer using the MALDI source Bruker SolariX 9.4T. Additionally, tandem MS (MS-MS) spectra were recorded using collision-induced dissociation. The laser was operated using a large laser focus (≈100 μm) and a laser power of 78% arbitrary units (a.u.), with 200 laser shots over 10 scans.

MALDI-TOF MS. High-throughput, single-cell MS was performed using a commercial MALDI mass spectrometer (AB Sciex 5800). The laser intensity was set to 4,300 a.u., with a laser repetition rate of 200 Hz and extraction time delay of 500 ns. A total of 70 subspectra were recorded for each spot, using a spiral pattern of ablation. The MALDI method used had a mass resolution of 9,200 (±750 [mean ± standard deviation]) for chlorophyll *a* and a mass accuracy of ±10 ppm.

Differentiating strains. To generate distinct profiles for the two *Chlamydomonas reinhardtii* strains CC-4346 (18) and CC-125, the two strains were spotted from separate cultures, each strain covering half of a microarray slide. Spotting a mixture of the strains covered a second microarray. Because a higher cell concentration was used in the mixture, the second microarray contained more spots with multiple cells.

Statistical analysis of mixed strains. The number of cells for each spot was determined by using fluorescence images of the microarray (excitation, 670 nm/emission, 630 nm). The spectra were divided into groups depending on the number of cells in the spot. The distribution of the chlorophyll *b*/chlorophyll *a* ratio was fitted using a kernel density estimation with the dfittool from MATLAB version 2014a (normal, automated bandwidth). The probability density function was then fitted with Gaussian distributions to account for the contribution of the wild-type strain CC-125. Since the chlorophyll *b*/chlorophyll *a* ratio in strain CC-4346 is zero due to the complete absence of chlorophyll *b*, the averaged signal of the two strains is fitted with a Gaussian distribution.

RESULTS

Single-cell sample preparation of microbial cells. Extracting the small amount of molecules from a microbial cell, which is surrounded by tough cell walls, is challenging. Most importantly, the extraction has to reproducibly extract a representative fraction of the contents of each cell. A schematic and fluorescence scans of the key steps during sample preparations are presented in Fig. 1. To minimize cross-contamination between adjacent spots on the microarray, the liquid handling was carried out using a contactless spotting device as described in Materials and Methods. The microarray slide has 1,430 spots that are each 300 μm in diameter and have a center-to-center distance of 720 μm. A detailed protocol of the spotting procedure can be found in Table S1 in the supplemental material. A very low number (2/1,430) of false-positive spectra, i.e., spots featuring a mass spectrometric signal reminiscent of a cell without a cell being present, indicated that cross-contamination is indeed negligible. Thanks to the orthogonal fluorescence detection of the autofluorescent chlorophyll, it can be visualized throughout the sample preparation process. Fluorescence detection allowed the lysis and extraction of the cells to be monitored. Moreover, contamination caused by early lysis in the

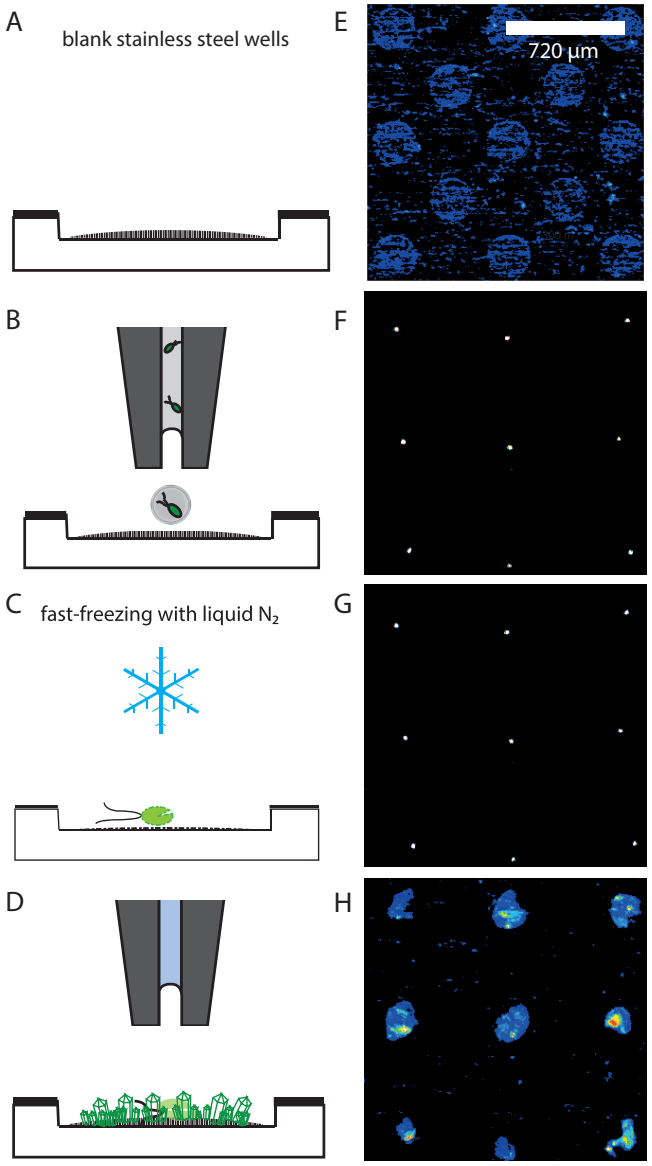

FIG 1 High-throughput microscale sample preparation for single-cell MALDI-MS. (A to D) Schematics of the individual steps of the workflow. (E to H) Confocal fluorescence scans of 9 wells on the microarray. (A, E) The cleaned, empty microarray slide has wells where the stainless steel surface is roughened up. (B, F) Cells are spotted from cell suspensions. Chlorophyll autofluorescence makes the cells clearly visible. (C, G) Fast freezing of the cells in liquid nitrogen leads to cell wall damage. (D, H) Chlorophyll and other soluble analytes are extracted from the cells by the matrix solution (10 mg/ml DHB in aqueous acetone). Evaporation of the solvent leads to cocrystallization of the extracted analytes with the MALDI matrix.

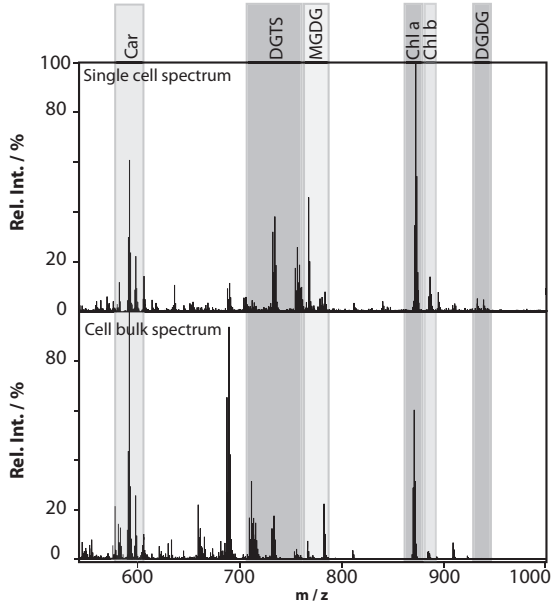

FIG 2 MALDI mass spectra obtained from a single *Chlamydomonas reinhardtii* cell and from cells in bulk on an FT-MS instrument. The single-cell mass spectrum is background corrected for better visibility of the peaks in the lower-mass region. This was achieved by subtracting the spectrum of an empty spot from the single-cell spectrum. Rel. Int., relative intensity; Car, carotenoids; Chl, chlorophyll.

medium or during the analyte extraction can be optically traced back. Our improved lysis procedure not only increased the percentage of successful single-cell measurements in MALDI-TOF MS to about 95% for the wild-type CC-125 but also boosted the signal-to-noise value of chlorophyll *a* in the spectra to a median of 540.

High-resolution MALDI-MS for peak identification. To assign the signals obtained in single-cell measurements using MALDI-time of flight (TOF) MS on *Chlamydomonas reinhardtii*, we used MALDI-FT-MS to determine their accurate mass (≤0.5 ppm mass deviation) and performed population-level MS-MS measurements (see Fig. S1 in the supplemental material), which matched those in the literature for *Chlamydomonas reinhardtii* (20, 21), allowing high confidence in the signal identification. A list of assigned compounds can be found in Table S2. Using the MALDI matrix DHB in the positive ion mode, the peaks identified from single-cell spectra can be assigned to different lipid classes, such as monogalactosyl-diacylglycerols (MGDG), digalactosyl-diacylglycerols (DGDG), or homoserine lipids (diacylglyceryl-*N*,*N*,*N*-trimethylhomoserine [DGTS]), or to chlorophylls. Chlorophylls are detected in the form of pheophytins due to the acidification of the extract during crystallization with the acidic DHB. The acidification leads to complete dissociation of Mg^{2+} from the porphyrin ring and, therefore, to the formation of the corresponding pheophytins (22). No intact chlorophylls are detected. Other major thylakoid lipid constituents, such as both sulfo- and phospholipids, can be detected on the single-cell level in negative-mode spectra using 9-aminoacridine (data not shown). Single-cell mass spectra show the same peak composition as spectra collected from cells in bulk, but they differ in relative composition (Fig. 2).

Characterization and identification of strains on the single-cell level. We used the new technique to distinguish two different strains of *Chlamydomonas reinhardtii* at the single-cell level. The distinction between the two strains was based on the presence or absence of a single compound, chlorophyll *b*: the wild-type strain CC-125 contains both chlorophyll *a* and *b*, while the chlorophyllide *a* oxidase insertional mutant CC-4346 contains chlorophyll *a* but lacks chlorophyll *b* (18). The absence of chlorophyll *b* in the mutant strains was verified both by MALDI-MS and by UV-VIS measurements on the population level (see Fig. S2 in the supplemental material). Single-cell spectra were recorded, producing a

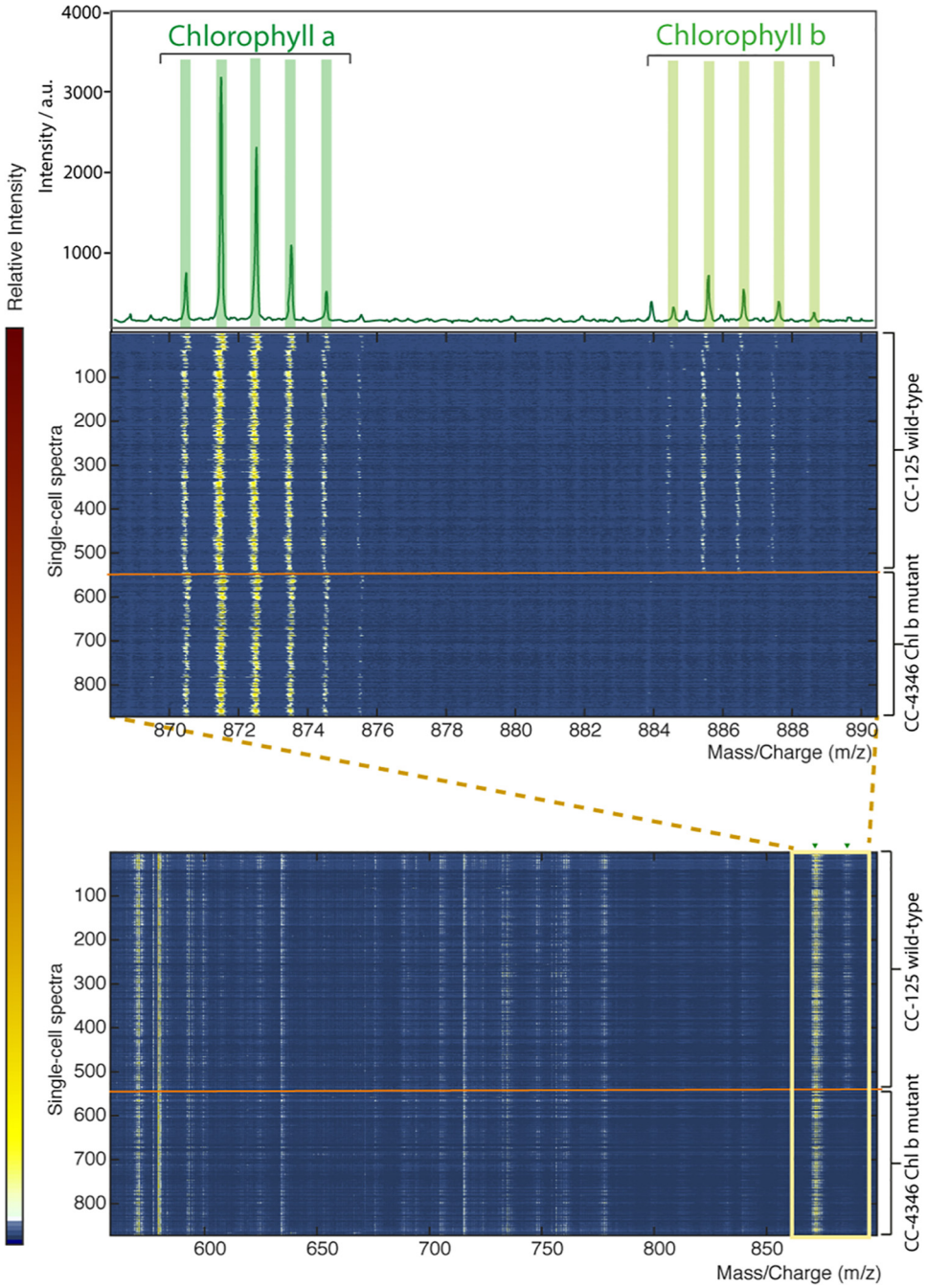

FIG 3 Single-cell mass spectra obtained from one measurement series. Spectra originate from two different strains of *Chlamydomonas reinhardtii*. CC-125 is a wild-type strain, while CC-4346 is a chlorophyll *b*-deficient mutant strain, reflected by the absence of the pheophytin *b* signal at 885.6 *m/z*. The visualization was achieved by using the msheatmap function in MATLAB. The midpoint value chosen was 0.99, which means that only the most intense 1% of signal values appear in the representation.

population profile for each strain. The cells were spotted and lysed on the array slide as described above. Seven hundred fifteen spots of each cell suspension were placed. In 541 spots, a single cell from strain CC-125 was found by fluorescence detection; 511 of these spots showed chlorophyll *a* signals in MALDI-MS. Single cells of strain CC-4346 were present in 332 spots, with 283 of these showing a chlorophyll *a* signal in MALDI-MS. The raw spectra are plotted as a heat map (MATLAB msheatmap function, midpoint-Value = 0.99) in Fig. 3. The background peaks caused by the MALDI matrix or contaminants are stable throughout the 1,430 spectra, as is clearly visible from the heat map. Furthermore, the strains can be easily distinguished based on the absence of chlorophyll *b* in CC-4346.

Deterioration of strain-specific phenotypes in multicell mass spectra. A key advantage of any single-cell-resolution technique is the distinct information it can supply in contrast to population

measurements. Therefore, we performed an experiment with a more concentrated cell suspension to see how the population profiles differ when looking at single cells and multicell spots. Interestingly, single-cell measurements from this run could be assigned to one of the two strains solely based on the mass spectrum. This is the first report on strain identification of single cells based on MS. Furthermore, spots that contain more than one cell show either distinct or mixed responses that can be attributed to contributions from one or both strains. The more cells per spot, the higher is the chance for a superimposed readout, as shown by the traces in Fig. 4. This emphasizes the ability of the method to perform real single-cell measurements and the detrimental effect of multicell measurements on the observation of population heterogeneity.

DISCUSSION

MALDI-MS of single cells allows the detection of abundant low-molecular-weight compounds with a polar character. The analytes identified from single-cell measurements in a widely used matrix (DHB) were mainly lipids belonging to different classes, such as thylakoid membrane lipids, membrane lipids, or pigments. The selectivity for these compounds can be attributed to their abundance, polarity, and solubility in the extractive solvent. The application of the MALDI matrix, which is dissolved in a solvent mixture, represents a liquid extraction from the cracked cells and helps to reduce the complexity of the biological background. Changing the extraction solvent or the matrix would therefore allow access to different analytes and change their relative contributions to the cell spectra obtained.

To maintain single-cell resolution, it is essential to prevent cross-contamination between spots. Both the noncontact microarrayer and the spacing of the microarray help to avoid cross-contamination. Only 2 of 453 empty wells showed MS signals reminiscent of cells in their spectra.

Another aspect of utmost importance for successful single-cell analysis is cell lysis. If the lysis process is not effectively controlled, the developmental state or nature of the cell wall will strongly influence the extraction. Thus, a bias for cells with a weakened cell wall due to changes in cell wall composition during, e.g., the cell cycle or aging would be introduced. Incomplete lysis can result in a poor or irreproducible mass spectrometric readout, since MALDI favors the ionization of the fraction that is cocrystallized with the matrix. Our system gives experimental evidence of this phenomenon, since fluorescence scanning after MALDI-MS shows significant fluorescence intensity for nonlysed cells (see Fig. S4 in the supplemental material). The orthogonal fluorescence information thus not only helps in optimizing the method but also helps to retrace the sources of errors.

The optimized lysis procedure also improves the spectral quality by increasing the percentage of single cells that yield a spectrum, the signal-to-noise values, and the number of analytes detected.

In many applications, MALDI-MS performs best by giving qualitative information. However, relative quantitative information can be obtained when the biological matrix background is reproducible. Since our method is label free, it delivers direct access to the phenotypes of individual cells. The composition of small molecules in individual cells of microbial populations can be used, e.g., to determine the penetrance of a mutation on the single-cell level. We therefore used the methods to differentiate cells of different strains based on single-cell mass spectra. *Chlamydomonas reinhardtii* mutant CC-4346, which is incapable of chlorophyll *b* biosynthesis (18), can be differentiated from the wild type by the absence of chlorophyll *b*. As predicted by population level MALDI-MS, as well as UV-VIS spectroscopy, there were no detectable levels of chlorophyll *b* in the knockout even when analyzed with single-cell resolution (see Fig. S3 in the supplemental material). A mixture of the wild-type and the mutant strain lacking chlorophyll *b* still showed distinct phenotypes in a mixed population. This was underlined by analyzing multicell measure-

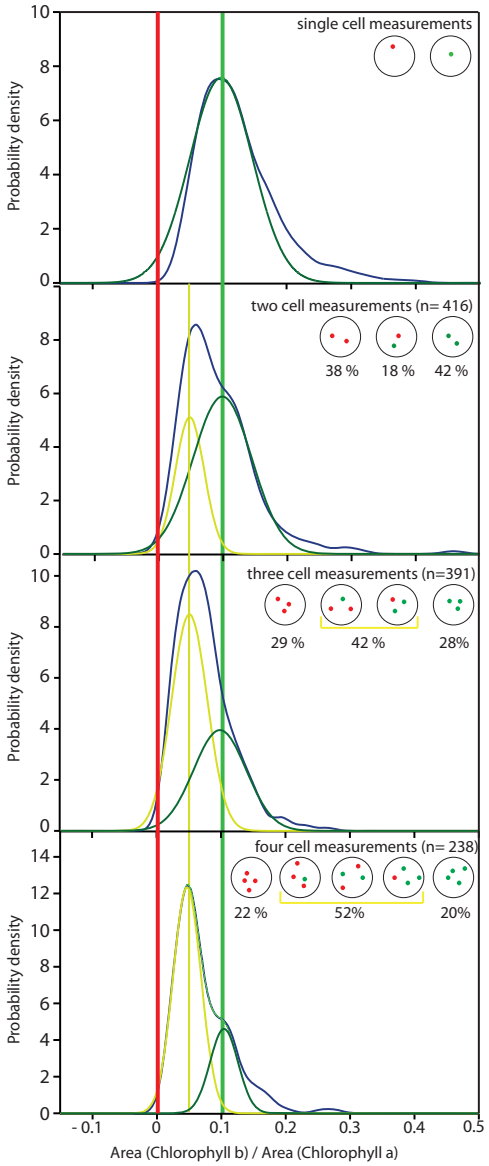

FIG 4 Probability densities of the chlorophyll *b*/chlorophyll *a* peak area ratios for spots containing 1 to 5 cells (dark blue trace). Single-cell distributions are averaged out (yellow trace) as the number of cells per measured spot increases. When single cells of the chlorophyll *b*-deficient strain CC-4346 (red) are measured, the chlorophyll *b*/chlorophyll *a* peak ratio is zero, while wild-type strain CC-125 (green) shows a ratio of around 0.1. The two strains can therefore easily be distinguished on the single-cell level. Measuring spots with more than one cell from mixed cultures leads to an intermediate response due to averaging of the two strain-specific responses. The effect is more pronounced the more cells are measured in one spot.

ments of the mixture of the two strains. Mixing the two strains caused the distinct spectral responses from the two strains to deteriorate rapidly with increasing numbers of cells measured, since both strains contribute to the spectra. This is an important validation of the experimental data that highlights the importance of real single-cell spectra for the characterization of molecular phenotypes present within a population. Since our experimental system represents an extreme case where the distinction is based on the presence or absence of a signal, this effect is expected to be more severe if the differences of the two phenotypes in the population are less pronounced, i.e., when distinctions are based on different amounts of a compound.

While recent publications have still included low-cell-number spectra (12), the newly developed high-throughput sample preparation method allows the measurement of pure single-cell profiles from microbial populations and their mixtures for the very first time. The quality and the flexibility of the single-cell measurements are highly promising concerning future applications of MALDI-MS for single-cell-resolution population analysis in microbiology.

ACKNOWLEDGMENTS

This work was financially supported by ETH Zurich.

Many thanks go to Rolf Brönnimann and Konstanins Jesimovs for the microstructuring of the microarray slides, Niklaus Amrhein and Stefan Hörtensteiner for their expertise and advice concerning *Chlamydomonas reinhardtii* and chlorophyll metabolism, Rolf Häfliger and Xiangyang Zhang for their help with the FT-MS measurements, and Carolin Blum, Lothar Opilik, Jacek Szcerbinski, Simon Weidmann, and Jan-Christoph Wolf for their support during data analysis and writing.

J.K and J.S conducted the experiments. J.K., R.F.S., S.R.F. and M.P. analyzed the results.

REFERENCES

1. **Dhar N, McKinney JD.** 2007. Microbial phenotypic heterogeneity and antibiotic tolerance. Curr Opin Microbiol **10:**30–38. http://dx.doi.org/10.1016/j.mib.2006.12.007.
2. **Brehm-Stecher BF, Johnson EA.** 2004. Single-cell microbiology: tools, technologies, and applications. Microbiol Mol Biol Rev **68:**538–559. http://dx.doi.org/10.1128/MMBR.68.3.538-559.2004.
3. **Buckling A, Harrison F, Vos M, Brockhurst MA, Gardner A, West SA, Griffin A.** 2007. Siderophore-mediated cooperation and virulence in Pseudomonas aeruginosa. FEMS Microbiol Ecol **62:**135–141. http://dx.doi.org/10.1111/j.1574-6941.2007.00388.x.
4. **Lidstrom ME, Konopka MC.** 2010. The role of physiological heterogeneity in microbial population behavior. Nat Chem Biol **6:**705–712. http://dx.doi.org/10.1038/nchembio.436.
5. **Blainey PC.** 2013. The future is now: single-cell genomics of bacteria and archaea. FEMS Microbiol Rev **37:**407–427. http://dx.doi.org/10.1111/1574-6976.12015.
6. **Eberwine J, Sul J-Y, Bartfai T, Kim J.** 2014. The promise of single-cell sequencing. Nat Methods **11:**25–27.
7. **Zenobi R.** 2013. Single-cell metabolomics: analytical and biological perspectives. Science **342:**1243259. http://dx.doi.org/10.1126/science.1243259.
8. **Davey HM, Winson MK.** 2003. Using flow cytometry to quantify microbial heterogeneity. Curr Issues Mol Biol **5:**9–15.
9. **Tanner S, Baranov V, Ornatsky O, Bandura D, George T.** 2013. An introduction to mass cytometry: fundamentals and applications. Cancer Immunol Immunother **62:**955–965. http://dx.doi.org/10.1007/s00262-013-1416-8.
10. **Nolan GP.** 2011. Flow cytometry in the post fluorescence era. Best Pract Res Clin Haematol **24:**505–508. http://dx.doi.org/10.1016/j.beha.2011.09.005.
11. **Amantonico A, Urban PL, Fagerer SR, Balabin RM, Zenobi R.** 2010. Single-cell MALDI-MS as an analytical tool for studying intrapopulation metabolic heterogeneity of unicellular organisms. Anal Chem **82:**7394–7400. http://dx.doi.org/10.1021/ac1015326.
12. **Ibáñez AJ, Fagerer SR, Schmidt AM, Urban PL, Jefimovs K, Geiger P, Dechant R, Heinemann M, Zenobi R.** 2013. Mass spectrometry-based metabolomics of single yeast cells. Proc Natl Acad Sci U S A **110:**8790–8794. http://dx.doi.org/10.1073/pnas.1209302110.
13. **Römpp A, Spengler B.** 2013. Mass spectrometry imaging with high resolution in mass and space. Histochem Cell Biol **139:**759–783. http://dx.doi.org/10.1007/s00418-013-1097-6.
14. **Zavalin A, Todd EM, Rawhouser PD, Yang J, Norris JL, Caprioli RM.** 2012. Direct imaging of single cells and tissue at sub-cellular spatial resolution using transmission geometry MALDI MS. J Mass Spectrom **47:**1473–1481. http://dx.doi.org/10.1002/jms.3108.
15. **Schober Y, Guenther S, Spengler B, Römpp A.** 2012. Single cell matrix-assisted laser desorption/ionization mass spectrometry imaging. Anal Chem **84:**6293–6297. http://dx.doi.org/10.1021/ac301337h.
16. **Watrous JD, Dorrestein PC.** 2011. Imaging mass spectrometry in microbiology. Nat Rev Microbiol **9:**683–694. http://dx.doi.org/10.1038/nrmicro2634.
17. **Goodenough UW, Heuser JE.** 1985. The Chlamydomonas cell wall and its constituent glycoproteins analyzed by the quick-freeze, deep-etch technique. J Cell Biol **101:**1550–1568. http://dx.doi.org/10.1083/jcb.101.4.1550.
18. **Tanaka A, Ito H, Tanaka R, Tanaka NK, Yoshida K, Okada K.** 1998. Chlorophyll a oxygenase (CAO) is involved in chlorophyll b formation from chlorophyll a. Proc Natl Acad Sci U S A **95:**12719–12723. http://dx.doi.org/10.1073/pnas.95.21.12719.
19. **Gorman DS, Levine RP.** 1965. Cytochrome f and plastocyanin: their sequence in the photosynthetic electron transport chain of Chlamydomonas reinhardi. Proc Natl Acad Sci U S A **54:**1665–1669. http://dx.doi.org/10.1073/pnas.54.6.1665.
20. **Giroud C, Gerber A, Eichenberger W.** 1988. Lipids of Chlamydomonas reinhardtii. Analysis of molecular species and intracellular site(s) of biosynthesis. Plant Cell Physiol **29:**587–595.
21. **Riekhof WR, Benning C.** 2009. Glycerolipid biosynthesis, p 41–68. *In* Harris EH, Stern DB, Witman GB (ed), The *Chlamydomonas* sourcebook, 2nd ed. Academic Press, London, United Kingdom. http://dx.doi.org/10.1016/B978-0-12-370873-1.00010-1.
22. **Lorenzen CJ.** 1967. Determination of chlorophyll and pheo-pigments: spectrophotometric equations. Limnol Oceanogr **12:**343–346. http://dx.doi.org/10.4319/lo.1967.12.2.0343.